Journal of Computer-Aided Molecular Design, **13:** 139–152, 1999.
KLUWER/ESCOM
© 1999 *Kluwer Academic Publishers. Printed in the Netherlands.*

Fractional description of free energies of solvation

F. Javier Luque[a,*], Xavier Barril[b] & Modesto Orozco[b,*]
[a]*Departament de Fisicoquímica, Facultat de Farmàcia, Universitat de Barcelona, Avgda Diagonal s/n, E-08028 Barcelona, Spain;* [b]*Departament de Bioquímica i Biologia Molecular, Facultat de Química, Universitat de Barcelona, Martí i Franquès 1, E-08028 Barcelona, Spain*

Received 7 April 1998; Accepted 20 August 1998

Key words: continuum models, hydrophilicity, hydrophobicity, partition coefficient, solvation free energy, transfer free energy

Summary

A new and rigorous method for the fractional description of solvation and transfer free energies is presented. The method is based on the use of the Miertus-Scrocco-Tomasi self-consistent reaction field method (MST-SCRF), and allows for a rigorous partition of the total solvation free energy into surface elements. The method gives a complete picture of the hydrophobicity/hydrophilicity of molecules. Present results allow us to expect that the method might provide useful information in drug design and molecular modeling studies.

Introduction

The relationship between the hydrophobic/hydrophilic character of molecules and their pharmacological activity has been known for decades [1–5], and descriptors of molecular solvation are among the most popular parameters in *quantitative structure-activity relationship* studies [1–5]. The connection between solvation and pharmacological activity can be explained at two levels. First, the drug needs to be soluble in a polar environment like blood, but it also has to pass through cellular membranes and other lipophilic barriers, which would be difficult for a very polar compound. Therefore, there must be a subtle balance between hydrophobic and hydrophilic properties. Second, the drug has to interact with a biological receptor, which implies that both drug and receptor have to be at least partially desolvated. This makes an important contribution to the binding free energy, and eventually to the pharmacological activity (see Figure 1).

The hydrophobic/hydrophilic character of a drug can be described by using parameters related to the transfer of the molecule from apolar and polar phases. The polar phase is usually water, and the apolar phase can be either gas phase or apolar solvents such as chloroform, carbon tetrachloride, hexane or octanol. In the first case the corresponding parameter is the free energy of hydration, while in the second it can be the transfer free energy or the partition coefficient [6].

Knowledge of hydrophobic/hydrophilic properties facilitates the understanding of drug transport and delivery. Such knowledge can be gained from general descriptors of the hydrophobic/hydrophilic nature of the whole molecule. Such a general description is less useful for the understanding of drug-receptor interactions. Receptor sites usually have hydrophobic pockets which bind the apolar parts of the drug, whereas its polar groups interact preferentially with hydrophilic sites. Accordingly, not only the global hydrophobic/hydrophilic character of the drug, but also the distribution pattern of hydrophobic and hydrophilic groups is important. The need for a complete 3-D representation of the hydrophobicity/hydrophilicity pattern of molecules [7–10] is, therefore, clear.

Approaches for the local representation of hydrophilicity/hydrophobicity are generally based on the use of fractional constants or atomic parameters [2, 11–25]. Within this approach the molecular hydrophilicity/hydrophobicity is divided into group contributions. This allows the a priori calculation of partition coefficients from empirical parameters representing contributions of molecular fragments to sol-

*To whom correspondence should be addressed.

vation. Furthermore, a rough representation of the molecular hydrophilic/hydrophobic properties in 3-D space is feasible. Thus, 3-D fractional methods compute the 'hydrophobicity' at a point j of the space using formalisms like that shown in Equation (1), where ξ_j describes the absolute or relative solvation at point *j*, and ζ_i is an empirical group descriptor of atom *i*. Different functions *f* have been used to represent the distance dependence of ξ (see for instance References 9 and 10).

$$\xi_j = \sum_{i=1}^{N} \zeta_i f(|R_i - R_j|). \quad (1)$$

The use of fractional constants has been criticized, since it relies on the assumption that the contribution of a given group to solvation is largely independent of its molecular environment. This has led to the development of methods that include correction terms (see References [19], [20], [22] and [24]) to account for neighboring influence on the solvation properties of groups. It is unclear whether or not these corrections are able to capture properly the complex and subtle 3-body effects involved in solvation.

An alternative to purely empirical methods for the calculation of absolute and relative solvation free energies is the use of *quasi*-empirical methods. These methods describe the hydrophobic/hydrophilic characteristics using a combination of empirical parameters and descriptors of molecular properties determined from quantum mechanical or classical calculations. Parameters that are used as descriptors are the molecular volume, the molecular electrostatic potential and the dipole moment [26–29].

Finally, theoretical methods provide an alternative way to obtain absolute and relative free energies of solvation. Within this approach the free energy of solvation is defined as the difference between the reversible works necessary to generate a molecule in the gas phase and in solution. Such works can be determined at the classical or quantum mechanical levels and using a discrete or macroscopic representation of the solvent (for review see [30–34]).

Continuum methods combine a discrete representation of the solute and a classical macroscopic treatment of the solvent [30, 32–35]. The methods based on a classical description of the solute are simple and computationally efficient [36–38], which make them very useful in drug-design studies and they have been incorporated in molecular modeling packages [39]. Furthermore, recent quantum-mechanical-continuum methods have been able to estimate solvation free energy for apolar solvents with an error of a few tenths of kcal/mol [40–43].

In this paper we present a partition scheme to divide the free energy of solvation into contributions assigned to surface elements which can in turn be integrated in order to derive atomic or group contributions. The method is based on the accurate polarizable continuum model (PCM) developed by Miertus-Scrocco and Tomasi (MST, [44], [45]), and on a rigorous partition of the free energy of solvation, which does not need any a posteriori correction. The new method provides 3-D pictures of the intrinsic solvation properties of molecules, which can be useful to describe the molecular hydrophobic/hydrophilic features.

Theoretical development

The MST method

The free energy of solvation (ΔG_{sol}) is determined by summing up three terms (Equation (2)): cavitation (ΔG_{cav}), van der Waals (ΔG_{vw}) and electrostatic (ΔG_{ele}). The cavitation term is the work required to generate the solute cavity in the solvent. The van der Waals contribution accounts for the free energy given by dispersion-repulsion interactions between solute and solvent. Finally, the electrostatic component is the work needed to build up the solute charge distribution in the solvent.

$$\Delta G_{sol} = \Delta G_{cav} + \Delta G_{vw} + \Delta G_{ele} \quad (2)$$

ΔG_{cav} is computed following Pierotti's scaled particle theory [46] adapted to cavities of molecular shape, [33, 47] so that the contribution of a given atom is weighted according to its exposure to the solvent. ΔG_{vw} is determined [48] using a linear relationship with the atomic surface as given by Equation (3), where the index i runs over atoms, the proportionality constant α stands for the atomic van der Waals parameter, and SAS is the atomic contribution to the solvent accessible surface.

$$\Delta G_{vw} = \sum_i \alpha_i \, SAS_i \quad (3)$$

ΔG_{ele} is determined assuming that the solvent is an infinite dielectric that reacts against the solute charge distribution generating a reaction field [44, 45]. Such a reaction field is coupled as a perturbation operator, V_R, to the gas phase Hamiltonian of the solute,

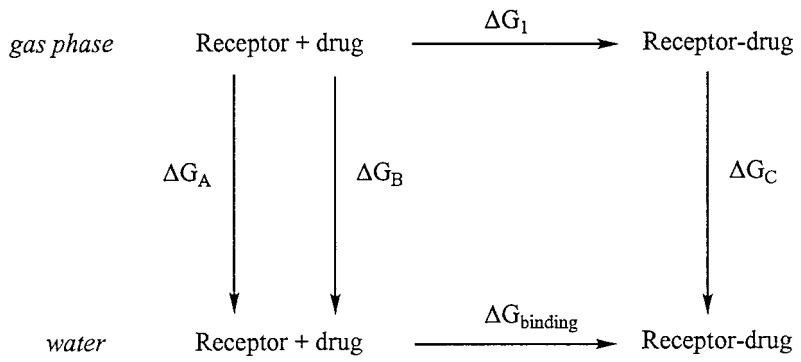

$$\Delta G_{binding} = \Delta G_1 + \Delta G_C - \Delta G_A - \Delta G_B = \Delta G_1 + \Delta\Delta G_{hyd}$$

Figure 1. Representation of the different terms contributing to the drug-receptor interaction in aqueous solution. ΔG_1 is the binding free energy in vacuum, and $\Delta G_{A,B,C}$ are the hydration free energies of the receptor, drug and drug-receptor complex.

H^0, leading to a pseudo-Schrödinger equation (Equation (4)),

$$(\hat{H}^0 + \hat{V}_R)\Psi = E\Psi. \tag{4}$$

The perturbation operator is given by Equation (5), where j stands for a small surface element (S) of the solute/solvent boundary, and Q_j (σ_j) denotes the charge (charge density) in the surface element S_j. The charge density is determined by solving Equation (6), where ε is the dielectric constant of the solvent, **n** is the normal vector to the element j of the surface, V is the electrostatic potential and the indexes σ and ρ refer to solvent and solute, respectively.

$$\hat{V}_R = \sum_{j=1}^{M} \frac{\sigma_j S_j}{|r_j - r|} = \sum_{j=1}^{M} \frac{Q_j}{|r_j - r|}, \tag{5}$$

$$\sigma_j = -\frac{\varepsilon - 1}{4\pi\varepsilon}\left(\frac{\delta(V_\sigma + V_\rho)}{\delta \mathbf{n}}\right). \tag{6}$$

Note the mutual dependence between the solute wavefunction and the solvent reaction field in Equations (4)–(6). This makes it necessary to resort to an iterative procedure to solve Equation (4) [44, 45]. Other strategies such as the closure solution, or the matrix inversion procedure have also been developed [33, 49–53]. ΔG_{ele} is then determined from Equation (7), where the indexes 0 and sol refer to gas phase and solvation.

$$\Delta G_{ele} = \left\langle \Psi^{sol}|\hat{H}^0 + \frac{1}{2}V^{sol}|\Psi^{sol}\right\rangle - \left\langle \Psi^0|\hat{H}^0|\Psi^0\right\rangle. \tag{7}$$

It has recently been shown [54–56] that the value of ΔG_{ele} can be accurately reproduced using Equation (8), where the solute is described by its gas phase wavefunction, Ψ^0, and $V^{sol}(\rho^{sol})$ stands for the solvent reaction field generated in presence of the fully polarized charge distribution (ρ^{sol}) of the solute in solution. The most remarkable feature of Equation (8) is that ΔG_{ele} is expressed only in terms of the solute-solvent interaction. Yet, it fully accounts for the polarization contribution to ΔG_{sol}.

$$\Delta G_{ele} = \left\langle \Psi^0|\frac{1}{2}V^{sol}(\rho^{sol})|\Psi^0\right\rangle. \tag{8}$$

Since the gas phase Hamiltonian is no longer needed for computing ΔG_{ele}, Equation (8) can be easily rewritten in a classical framework as given by Equation (9) [57–59], which will be referred to as *quasi*-classical approach. In Equation (9) Q_j^{vac} accounts for the ESPF (electrostatic-potential and field fitted charges; see [57]) charges that represent the solute charge distribution in vacuo, N is the number of atomic charges, q_j^{sol} stands for the charge associated with the surface element j generated in response to the fully polarized charge distribution of the solute in solution, and M is the number of surface elements

$$\Delta G_{ele} = \frac{1}{2}\sum_{i=1}^{N} Q_i^{vac} V^{sol}(\rho^{sol}) = \frac{1}{2}\sum_{i=1}^{N}\sum_{j=1}^{M} \frac{Q_i^{vac} q_j^{sol}}{|r_i - r_j|}. \tag{9}$$

MST calculations can be performed at different quantum mechanical levels of theory [48, 60–65]. The parametrized MST versions estimate ΔG_{sol} in water and several apolar solvents with average errors below 1 kcal/mol for neutral molecules [42, 43, 62, 64, 65]. There are many examples in the literature showing the successful application of the MST method in the study of chemical and biochemical systems in solution (see [30] and [33] for review). The reliability of Equation (8) in reproducing accurately the values of ΔG_{ele} (Equation (7)) has also been shown at the SCF level [54–56]. Finally, the goodness of the *quasi*-classical approach given by Equation (9) has also been demonstrated [54, 57, 58].

Partitioning of ΔG_{sol} in the MST method

The cavitation and van der Waals components of ΔG_{sol} can be easily decomposed into atomic contributions, since they depend on the exposure of atoms to the solvent. Unfortunately, since the solvent (modeled as point charges distributed over the cavity surface) interacts with the whole charge distribution of the solute, partitioning of the electrostatic term (Equation (7)) is not so simple. However, the use of Equation (8) allows us to express the electrostatic term as the addition of contributions arising from the solute/solvent interaction at all the surface elements (ΔG^{j}_{ele}; Equation (10)).

$$\Delta G_{ele} = \sum_{j=1}^{M} \Delta G^{j}_{ele} = \frac{1}{2} \sum_{j=1}^{M} q^{sol}_{j} \left\langle \Psi^{0} \left| \frac{1}{r_j - r} \right| \Psi^{0} \right\rangle \qquad (10)$$

Since the surface elements can be assigned to the atoms in the solute, Equation (10) can be rewritten as shown in Equation (11), where the electrostatic contribution of a given atom (ΔG^{i}_{ele}) is determined considering the interaction of the solute charge distribution with the surface elements pertaining to the surface generated by such an atom.

$$\Delta G_{ele} = \sum_{j=1}^{N} \Delta G^{i}_{ele} = \frac{1}{2} \sum_{j=1}^{N} \sum_{j=1}^{M \in N} q^{sol}_{j} \left\langle \Psi^{0} \left| \frac{1}{r_j - r} \right| \Psi^{0} \right\rangle \qquad (11)$$

If the solute charge distribution is treated by means of a set of N_q point charges, Q^{vac}_{k} (k=1,..,N_q), Equation (12) gives the classical expression of Equation (11). Let us note that N_q is not necessarily equal to the number of atoms in the molecule.

$$\Delta G_{ele} = \sum_{i=1}^{N} \Delta G^{i}_{ele} = \frac{1}{2} \sum_{i=1}^{N} \sum_{j=1}^{M \in N} \sum_{k=1}^{N_q} \left| \frac{Q^{vac}_{k} q^{sol}_{j}}{r_k - r_j} \right|. \qquad (12)$$

The contribution to the free energy of solvation associated with the surface of every atom (ΔG^{i}_{sol}) can then be derived by adding the van der Waals, cavitation and electrostatic terms (Equation (13)).

$$\Delta G^{i}_{sol} = \sum_{i=1}^{N} \Delta G^{i}_{cav} + \sum_{i=1}^{N} \Delta G^{i}_{vw} + \sum_{i=1}^{N} \Delta G^{i}_{ele}. \qquad (13)$$

It is worth stressing that the 'atomic' contribution (ΔG^{i}_{sol}) to ΔG_{sol} should be understood as the contribution of the solute associated with the solvent-exposed surface of atom i, and not really as the contribution of atom i to ΔG_{sol}. Then, these parameters differ from those derived by Cramer and Truhlar with the AMSOL-Generalized-Born-Approach [66–69]. Keeping this in mind, the atomic contributions to the free energy of transfer between two solvents, ω and τ, can be determined from Equation (14), where different cavity definitions can be used for the two solvents.

$$\Delta G^{\omega \to \tau}_{transfer} = \sum_{i=1}^{N} \Delta\Delta G^{i}_{cav} + \sum_{i=1}^{N} \Delta\Delta G^{i}_{vw} + \sum_{i=1}^{N} \Delta\Delta G^{i}_{ele}, \qquad (14)$$

where

$$\Delta\Delta G = \Delta G(\tau) - \Delta G(\omega).$$

Computational details

Free energies of solvation were computed at the ab initio HF/6-31G(d) and AM1 levels using our optimized versions [48, 62–65] of the MST method [44, 45]. AM1 and HF/6-31G(d) optimized geometries were used. Ab initio calculations were performed with MonsterGauss [70]. Semi-empirical and *quasi*-classical calculations were carried out using a modified version of MOPAC [71]. ESP and ESPF charges were determined using MOPETE/MOPFIT [72]. Graphical display was performed with INSIGHT-II [73]. Calculations were carried out on the ORIGIN-2000 of the Centre de Supercomputació de Catalunya (CESCA), as well as on workstations in our laboratory.

Results and discussion

Suitability of the fractional approach

Before examining the suitability of the partitioning scheme, it is necessary to check the reliability of the results provided by Equations (10)–(11). For this purpose the free energies of hydration of 33 derivatives of benzene (Table 1) were determined at the quantum mechanical (QM) HF/6-31G(d) level using those expressions, and the results were compared with the exact MST-SCRF values computed from Equations (2) and (7). Figure 2 clearly shows that Equations (11) and (13), and Equations (2) and (7) give identical results. This means that numerical errors in the definition of the cavity and errors arising from Equation (8) are both negligible.

Suitability of the fractional quasi-classical approach

It is also worth examining the reliability of the partitioning scheme based on the *quasi*-classical approach (Equation (12)), since it can be useful for the study of very large molecules of potential biochemical or pharmacological interest. In this case the free energies of hydration for the derivatives of benzene were determined from Equation (12) (ESPF charges determined at the HF/6-31G(d) level were used in calculations) and compared with the exact MST-SCRF values. Figure 3 shows that the *quasi*-classical approach introduces some uncertainties in the results, probably due to the simplified representation of the solute charge distribution. Nevertheless, the error lies within the uncertainty of any SCRF calculation (typically around 1 kcal/mol for free energies of hydration).

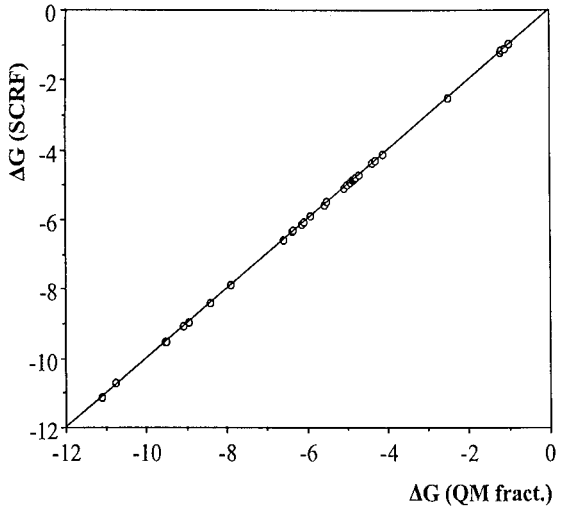

Figure 2. Relationship between the free energies of hydration (kcal/mol) determined using the rigorous QM HF/6-31G(d) method (Equations (2) and (7)) and the QM HF/6-31G(d) fractional approach (Equations (11) and (13)). The statistical parameters of the comparison are: root-mean square error = 0.0 kcal/mol; mean signed error = 0.0 kcal/mol; regression equation y = 1.00 × (r^2 = 1.00).

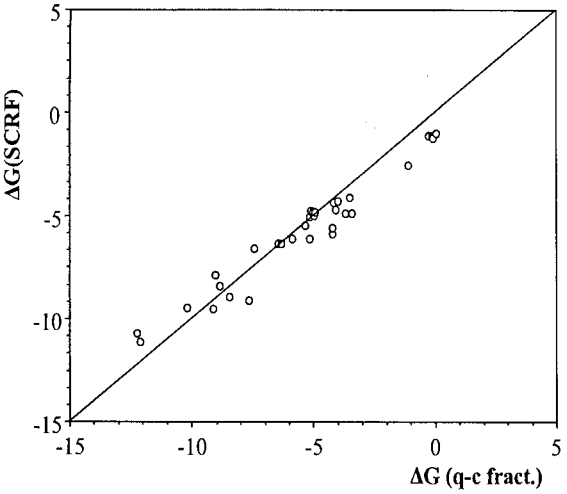

Figure 3. Relationship between the free energies of hydration (kcal/mol) determined using the rigorous QM HF/6-31G(d) method (Equations (2) and (7)) and the *quasi*-classical 6-31G(d) fractional approach (Equations (12) and (13)). The statistical parameters of the comparison are: root-mean square error = 0.8 kcal/mol; mean signed error = 0.3 kcal/mol; regression equation y = 1.00 × (r^2 = 0.96).

Table 1. Fractional free energies of hydration (kcal/mol) for derivatives of benzene computed at the QM HF/6-31G(d) and AM1 levels

Core	R_1	R_2	R_3	R_4	HF/6-31G(d)			AM1		
					ΔG(core)	$\Delta G(R_1)$	$\Delta G(R_{2,3,4})$	ΔG(core)	$\Delta G(R_1)$	$\Delta G(R_{2,3,4})$
C6H5	COCH3				−0.88	−5.01		−0.99	−4.50	
C6H5	NH2				−1.08	−3.90		−1.48	−4.24	
C6H5	COH				−0.97	−4.60		−0.93	−3.70	
C6H5	CONH2				−1.01	−8.51		−1.18	−9.57	
C6H5	H				−1.21	0.10		−1.01	0.11	
C6H5	COOH				−0.65	−5.71		−0.83	−6.40	
C6H5	COCH2COMe				−1.56	−7.51		−1.46	−6.16	
C6H5	CN				−1.69	−4.43		−1.07	−2.11	
C6H5	CH2NH2				−1.04	−3.67		−1.29	−3.91	
C6H5	CH2CH3				−1.61	0.62		−1.64	0.57	
C6H5	OEt				−0.91	−1.60		−1.12	−1.74	
C6H5	OH				−0.88	−3.90		−1.05	−3.48	
C6H5	CH3				−1.47	0.36		−1.38	0.34	
C6H5	COOMe				−0.45	−4.11		−0.93	−3.80	
C6H5	NO2				−2.00	−3.50		−2.11	−3.78	
C6H4	OH		CH3		−0.93	−4.03	0.16	−1.21	−3.57	0.13
C6H4	NO2		NH2		−1.52	−3.04	−3.84	−1.53	−4.28	−5.03
C6H4	NO2		COOH		−2.38	−1.81	−5.32	−2.79	−2.58	−5.63
C6H4	OMe	OH			−0.53	−0.25	−3.52	−0.81	−0.70	−2.65
C6H4	OH	COOH			−0.61	−1.35	−4.62	−0.84	−0.87	−5.23
C6H4	NH2	COOH			−0.71	−2.00	−5.19	−1.04	−2.53	−5.80
C6H4	OH	CH3			−0.80	−3.21	−0.12	−0.96	−2.58	−0.06
C6H4	NO2	CH3			−1.49	−3.38	0.00	−1.64	−4.11	−0.03
C6H4	O-Me	COOH			−1.18	−1.02	−6.74	−1.43	−1.21	−7.11
C6H4	NO2	NH2			−2.29	−3.29	−0.76	−1.48	−4.48	−3.52
C6H4	NO2	OH			−1.78	−1.43	−1.18	−1.88	−2.40	−1.49
C6H4	CH3	CH3			−1.77	0.30	0.30	−1.81	0.26	0.26
C6H4	OMe			OH	−0.72	−1.45	−3.90	−1.08	−1.62	−3.48
C6H4	NH2			COOH	−0.80	−3.65	−6.67	−1.05	−4.58	−7.01
C6H4	OH			CH3	−0.92	−4.15	0.25	−1.23	−3.60	0.21
C6H4	NO2			NH2	−1.67	−4.99	−4.10	−1.45	−5.70	−5.36
C6H4	NH2			CH3	−1.29	−4.16	0.37	−1.91	−4.35	0.36
C6H4	CH3			CH3	−1.90	0.34	0.34	−1.87	0.32	0.33

Suitability of the semiempirical fractional approach

Another point that deserves attention is the suitability of the partitioning scheme within semiempirical calculations. It must be emphasized that Equation (8) is rigorous only at the ab initio level, but not at the semiempirical one, since the definition of the one-electron integrals involving the perturbation operator in Equations (4) and (6) is not unique (see for instance [70]). However, since semiempirical methods, especially AM1 [71] and PM3 [72], are very popular in studies of biomolecules, we also tested the suitability of the partitioning scheme at the AM1 level.

The AM1 fractional free energies of solvation (in water and chloroform) for derivatives of benzene are given in Tables 1 and 2, and comparison with the HF/6-31G(d) values is shown in Figure 4. The results show that, at least qualitatively, the AM1 method provides reasonable estimates in the two solvents. Semiempirical calculations, even though less rigorous than the ab initio ones, are a useful and inexpensive alternative for examining the solvation properties in large molecules, especially when series of structurally related molecules are considered.

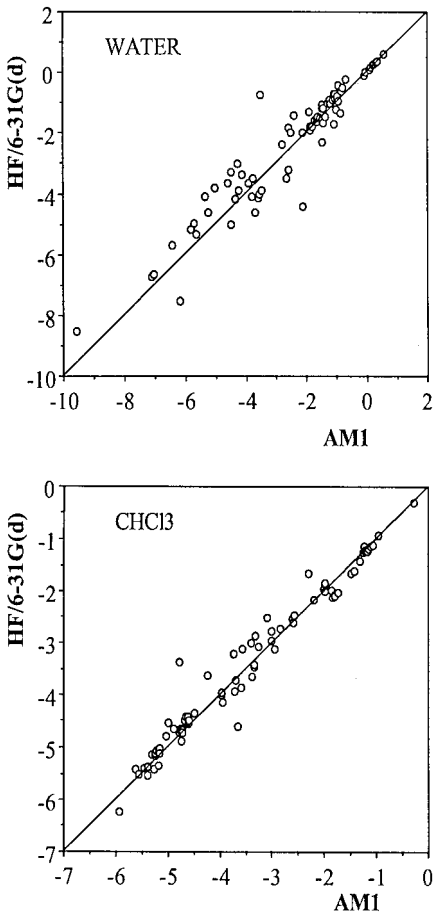

Figure 4. Relationship between the QM HF/6-31G(d) and AM1 fractional free energies of solvation in water and chloroform (kcal/mol) for benzene derivatives. All values were determined at the QM fractional level (Equations (11) and (13)). The statistical parameters of the comparison are: (a) water: root-mean square error = 0.6 kcal/mol; mean signed error = 0.1 kcal/mol; regression equation y = 0.93 × (r^2 = 0.92); (b) chloroform: root-mean square error = 0.3 kcal/mol; mean signed error = 0.1 kcal/mol; regression equation y = 0.98 × (r^2 = 0.96).

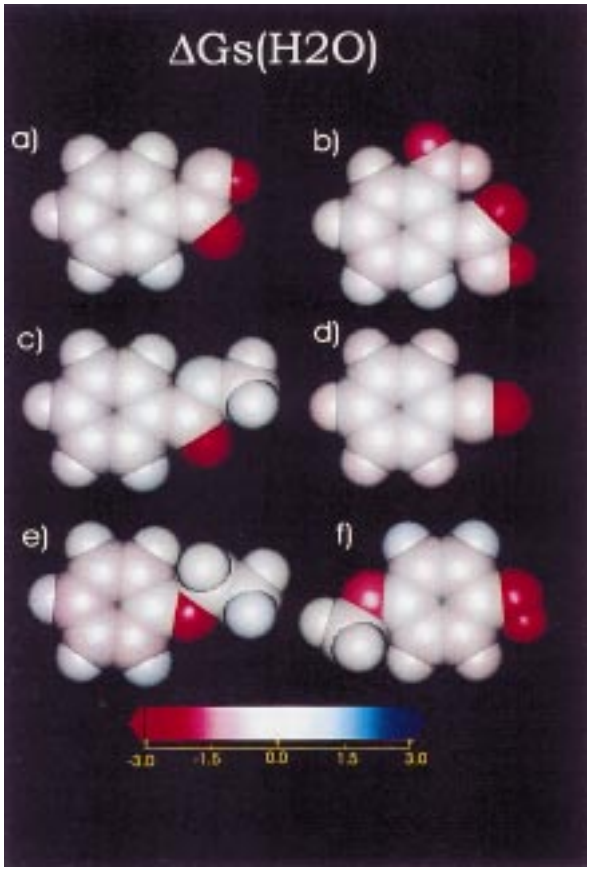

Figure 5. Fractional free energies of hydration determined at the QM HF/6-31G(d) fractional level for (a) C_6H_5COOH, (b) *o*-$NH_2C_6H_4COOH$, (c) C_6H_5COOMe, (d) C_6H_5CN, (e) C_6H_5OEt and (f) $MeOC_6H_4OH$. Color code is in kcal/mol.

Substituent fractional free energies of solvation

The results in Table 1 allow us to determine the fractional hydration of different functional groups. As expected, increasing the polarity of the substituent leads to more negative fractional free energies of hydration. The contribution of a given group clearly depends on the environment around the molecule. Thus, the value of the hydroxyl group ranges in most cases from −3 to −4 kcal/mol; however, it is around −1 kcal/mol when there are carboxy or nitro groups in its vicinity. Substituents lead to moderate, but significant changes in the fractional contribution of the benzene ring. These subtle changes are difficult to predict, since polar groups like the −OH decrease the contribution of the aromatic ring, while apolar groups like $-C_2H_5$ show the opposite trend. Finally, the change in the fractional contribution for a given group depending on the position (ortho, meta, para) in the benzene ring is also clear. Thus, the contribution of the methyl group attached to phenol varies from −0.12 to 0.16 to 0.25 for ortho, meta and para substitutions, and the hydroxyl contribution changes from −3.21 to −4.03 to −4.15, respectively. Larger changes are found in other cases, like the amino group attached to nitrobenzene, whose contribution varies from −0.76 (ortho) to −4.10 (para).

A fine representation of the solvation can be achieved from graphical display of atomic fractional solvation free energies. Figure 5 shows the hydration contributions computed at the ab initio QM level (Equation (11)) for selected molecules. The surface re-

Table 2. Fractional free energies of solvation in chloroform (kcal/mol) for derivatives of benzene computed at the QM HF/6-31G(d) and AM1 levels

Core	R_1	R_2	R_3	R_4	HF/6-31G(d)			AM1		
					ΔG(core)	$\Delta G(R_1)$	$\Delta G(R_{2,3,4})$	ΔG(core)	$\Delta G(R_1)$	$\Delta G(R_{2,3,4})$
C6H5	COCH3				−5.06	−3.73		−5.19	−3.70	
C6H5	NH2				−5.37	−2.47		−5.39	−2.57	
C6H5	COH				−5.16	−3.11		−5.24	−2.94	
C6H5	CONH2				−5.06	−5.12		−5.23	−5.24	
C6H5	H				−5.52	−0.30		−5.56	−0.27	
C6H5	COOH				−5.02	−3.93		−5.17	−3.72	
C6H5	COCH2COMe				−5.51	−6.24		−5.55	−5.93	
C6H5	CN				−5.53	−3.64		−5.40	−3.38	
C6H5	CH2NH2				−5.11	−2.77		−5.16	−3.01	
C6H5	CH2CH3				−5.35	−1.98		−5.19	−1.85	
C6H5	OEt				−5.40	−2.61		−5.45	−2.59	
C6H5	OH				−5.38	−2.03		−5.39	−1.73	
C6H5	CH3				−5.41	−1.18		−5.26	−1.14	
C6H5	COOMe				−5.14	−3.95		−5.31	−3.58	
C6H5	NO2				−5.41	−3.11		−5.63	−3.58	
C6H4	OH		CH3		−4.71	−2.09	−1.25	−4.79	−1.79	−1.26
C6H4	NO2		NH2		−4.41	−3.21	−2.95	−4.66	−3.75	−3.01
C6H4	NO2		COOH		−4.53	−2.87	−3.87	−5.00	−3.32	−3.60
C6H4	OMe	OH			−4.67	−1.95	−1.64	−4.73	−2.00	−1.48
C6H4	OH	COOH			−4.49	−1.11	−3.42	−4.68	−1.06	−3.34
C6H4	NH2	COOH			−4.54	−1.84	−3.47	−4.60	−1.98	−3.34
C6H4	OH	CH3			−4.66	−1.61	−1.42	−4.74	−1.42	−1.32
C6H4	NO2	CH3			−4.64	−3.01	−1.22	−4.88	−3.41	−1.20
C6H4	OMe	COOH			−4.43	−1.99	−4.00	−4.62	−1.99	−3.98
C6H4	NO2	NH2			−3.38	−4.61	−1.64	−4.78	−3.66	−2.30
C6H4	NO2	OH			−4.79	−2.51	−0.93	−5.03	−3.10	−0.97
C6H4	CH3	CH3			−4.89	−1.14	−1.14	−4.75	−1.10	−1.23
C6H4	OMe			OH	−4.65	−2.16	−2.12	−4.77	−2.20	−1.84
C6H4	NH2			COOH	−4.35	−2.73	−4.15	−4.50	−2.85	−3.95
C6H4	OH			CH3	−4.68	−2.08	−1.22	−4.76	−1.79	−1.23
C6H4	NO2			NH2	−4.49	−3.62	−3.06	−4.59	−4.25	−3.25
C6H4	NH2			CH3	−4.73	−2.53	−1.20	−4.73	−2.61	−1.21
C6H4	CH3			CH3	−4.56	−1.24	−1.24	−4.62	−1.22	−1.18

gions making larger contributions to ΔG_{hyd} are those enclosing polar groups. The ability to distinguish the contribution of two identical atoms in different environments is also remarkable. For instance, in benzoic acid the region surrounding the hydroxyl oxygen contributes to ΔG_{hyd} less than the region surrounding the carbonyl oxygen. Similarly, in *o*-amino benzoic acid the *trans* amino hydrogen contributes more to the total hydration than the *cis* amino one. Finally, it is also clear that the contribution to ΔG_{hyd} of the oxygen atom in an hydroxyl group is larger than that of an ether oxygen.

Substituent fractional partition coefficients

Fractional contributions to transfer free energies or partition coefficients can be easily determined with the preceding partitioning scheme. Ab initio and semiempirical results for the transfer between chloroform and water are given in Table 3. In all cases the contribution to the partition coefficient of the benzene ring is positive, in agreement with the expected hydrophobic-

Table 3. Fractional partition coefficients for derivatives of benzene computed at the QM HF/6-31G(d) and AM1 levels

Core	R_1	R_2	R_3	R_4	HF/6-31G(d)			AM1		
					ΔG(core)	$\Delta G(R_1)$	$\Delta G(R_{2,3,4})$	ΔG(core)	$\Delta G(R_1)$	$\Delta G(R_{2,3,4})$
C6H5	COCH3				3.06	−0.95		3.08	−0.59	
C6H5	NH2				3.14	−1.04		2.87	−1.22	
C6H5	COH				3.07	−1.09		3.16	−0.56	
C6H5	CONH2				2.97	−2.49		2.97	−3.18	
C6H5	H				3.16	0.30		3.34	0.28	
C6H5	COOH				3.21	−1.30		3.18	−1.96	
C6H5	COCH2COMe				2.90	−0.93		3.00	−0.17	
C6H5	CN				2.82	−0.59		3.17	0.93	
C6H5	CH2NH2				2.99	−0.66		2.84	−0.66	
C6H5	CH2CH3				2.75	1.91		2.60	1.78	
C6H5	OEt				3.30	0.74		3.17	0.63	
C6H5	OH				3.30	−1.37		3.18	−1.28	
C6H5	CH3				2.88	1.13		2.84	1.08	
C6H5	COOMe				3.44	−0.12		3.21	0.13	
C6H5	NO2				2.50	−0.29		2.58	−0.14	
C6H4	OH		CH3		2.77	−1.43	1.04	2.63	−1.31	1.02
C6H4	NO2		NH2		2.11	0.12	−0.65	2.30	−0.39	−1.48
C6H4	NO2		COOH		1.58	0.78	−1.07	1.63	0.54	−1.49
C6H4	OMe	OH			3.04	1.25	−1.38	2.88	0.95	−0.86
C6H4	OH	COOH			2.85	−0.18	−0.89	2.81	0.13	−1.38
C6H4	NH2	COOH			2.81	−0.12	−1.26	2.61	−0.41	−1.80
C6H4	OH	CH3			2.84	−1.17	0.95	2.77	−0.85	0.92
C6H4	NO2	CH3			2.31	−0.27	0.89	2.37	−0.51	0.86
C6H4	OMe	COOH			2.39	0.71	−2.01	2.34	0.58	−2.30
C6H4	NO2	NH2			0.79	0.97	0.64	2.42	−0.60	−0.90
C6H4	NO2	OH			2.21	0.79	−0.18	2.31	0.52	−0.38
C6H4	CH3	CH3			2.29	1.06	1.06	2.15	1.00	1.02
C6H4	OMe			OH	2.88	0.52	−1.31	2.70	0.43	−1.21
C6H4	NH2			COOH	2.61	−0.68	−1.85	2.53	−1.27	−2.24
C6H4	OH			CH3	2.75	−1.52	1.08	2.59	−1.33	1.05
C6H4	NO2			NH2	2.07	−1.00	−0.77	2.30	−1.06	−1.55
C6H4	NH2			CH3	2.53	−1.20	1.16	2.07	−1.27	1.15
C6H4	CH3			CH3	1.95	1.16	1.16	2.01	1.13	1.11

ity of the aromatic core. Regions around polar groups contribute more to the solvation in water than they do in chloroform, while the reverse trend is found for regions surrounding apolar groups. The relevance of the chemical environment in determining the fractional contribution to the partition coefficient is also clear. For instance, the contribution arising from the surface around a hydroxyl group is typically −1.3 to −1.4, but in some cases it is around zero. Therefore, the use of empirical group fractional parameters can lead to an erroneous description of the hydrophobicity around the molecule.

A graphical display of the fractional contributions to the chloroform/water transfer free energy for selected benzene derivatives is shown in Figure 6. As expected, the most hydrophobic regions are the aromatic ring and aliphatic groups. Nevertheless, not all the aromatic ring shows the same hydrophobicity, since those regions around substituted carbons are usually less hydrophobic than the rest of the benzene core. It is also worth noting that areas around polar groups such as the amino can not be very hydrophilic as a consequence of the chemical environment of the group. Similarly, the hydrophilicity around an hy-

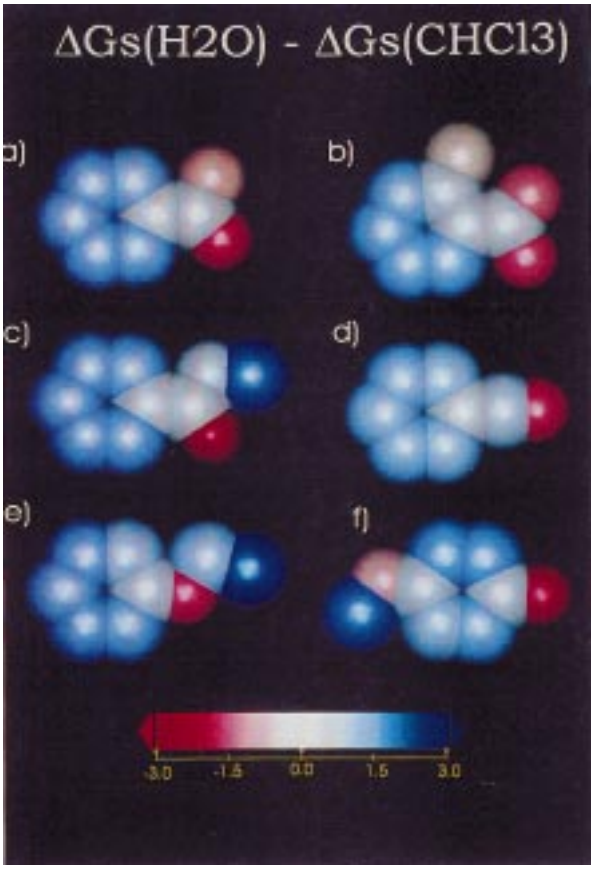

Figure 6. Fractional chloroform/water transfer free energies determined at the QM HF/6-31G(d) fractional level for (a) C_6H_5COOH, (b) *o*-$NH_2C_6H_4COOH$, (c) C_6H_5COOMe, (d) C_6H_5CN, (e) C_6H_5OEt and (f) $MeOC_6H_4OH$. Molecules are represented using an united-atom model. Blue (red) color means preferential solvation in chloroform (water). Color code is in kcal/mol.

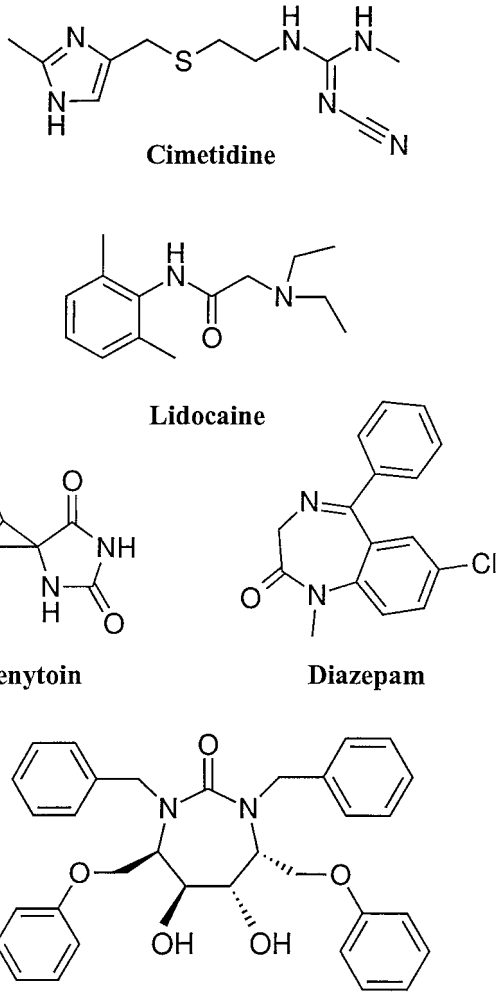

Figure 7. Chemical structures of selected drugs.

droxyl group can be strongly affected by its chemical environment (compare for instance compounds a and d). As noted before, it is difficult that these subtle differences can be captured by empirical models based on fittings to data bases containing partition coefficients of thousands of molecules.

The fractional contributions to the chloroform/water transfer free energy for a series of representative drugs were also determined at the *quasi*-classical level (see Figure 7). The results in Figure 8 demonstrate the ability of the method to obtain 3D pictorial representations of the hydrophobic characteristics of drugs. Thus, in cimetidine the center of the molecule, especially the sulfur atom, is more hydrophobic, while the imidazole and cyanoguanidine moieties are more hydrophilic. The large amphipatic character of phenytoin and the large anisotropy of the hydrophilic/hydrophobic distribution of lidocaine and diazepam are also clear. Figure 9 displays the fractional contribution to the chloroform/water transfer free energy of the cyclic urea inhibitor AHA001 (see also Figure 7). The molecule is mostly hydrophobic, especially in the outermost part, due to the presence of benzene groups. This explains why this drug interacts so deeply into the recognition site of the HIV protease (see [77] and Figure 9). In fact, the only polar region in Figure 9 (around the carbonyl oxygen) is hydrogen-bonded to an amino group of the protein, while all the apolar groups establish hydrophobic contacts with residues of the protein.

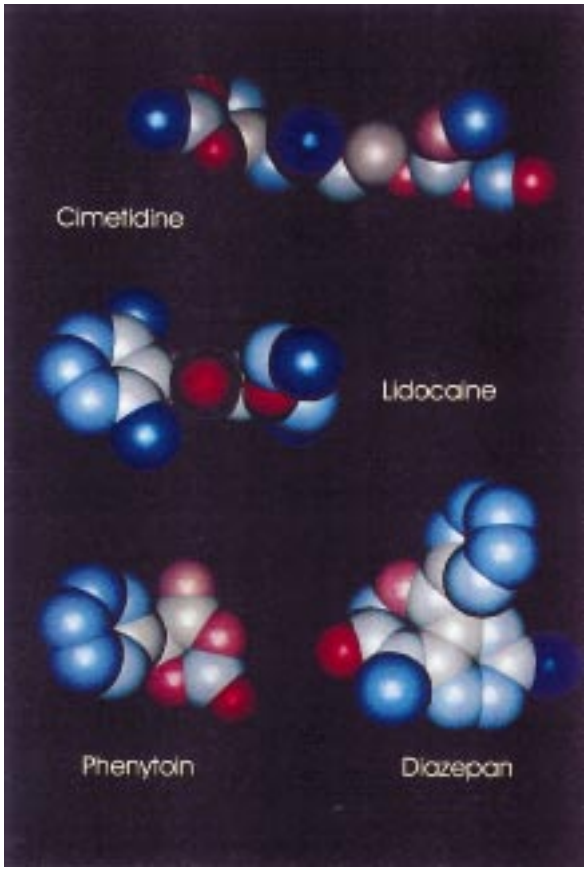

Figure 8. Fractional chloroform/water transfer free energies determined at the AM1 *quasi*-classical level for the drugs shown in Figure 7. Blue (red) color means preferential solvation in chloroform (water). Color code is in kcal/mol.

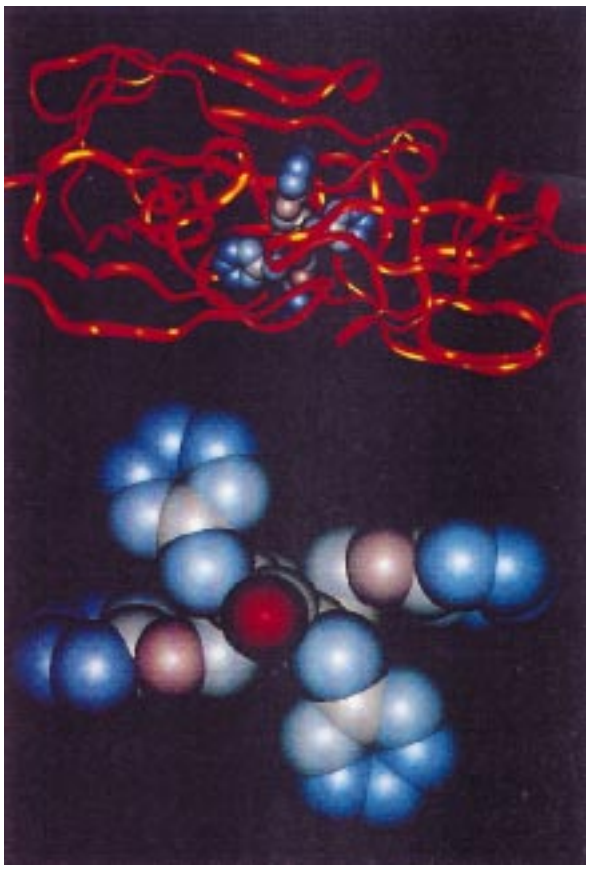

Figure 9. Top: crystal structure of the HIV-protease:AHA001 complex. Bottom: Fractional chloroform/water transfer free energies determined at the AM1 *quasi*-classical level for the cyclic urea inhibitor (AHA001; see Figure 7). Color code is in kcal/mol.

Comparison with empirical fractional parameters

Our approach to computing fractional estimates of solvation and transfer free energies is based on the partition of ΔG_{sol} into surface elements, which can be added to determine atomic or group contributions. In general, empirical fractional transfer parameters give an approximate picture of the hydrophobicity/hydrophilicity of a group. This can be seen in Figure 10, which shows that the QM HF/6-31G(d) fractional estimates of chloroform/water partition coefficients (relative to benzene) reproduce reasonably the variation in the experimental π (octanol/water) values. The regression equation (see legend to Figure 10) shows that the computed fractional contributions tend to be twice the value of the π, which reflects the difference in dielectric response between octanol and chloroform [78]. This supports the ability of our model to describe the hydrophobic/hydrophilic properties of molecules.

We must emphasize, however, that our method does not intend to provide another estimate of group contributions to solvation or transfer free energies. In fact, such a partition is not rigorously feasible. On the contrary, our method allows to partition the solvation (or transfer) free energy into surface elements, which can then be added to define how much of the solvation/transfer free energy is due to the solute-solvent interaction occurring in the vicinity of one atom or group of atoms. Both concepts are clearly different and should not be confused.

A clear example of the difference between the empirical fractional approach and our method is illustrated by the results given in Table 4 (see also Figure 11), which allows us to compare the fractional free energies of solvation for the benzene molecules in the stacked dimer and trimer with regard to the free

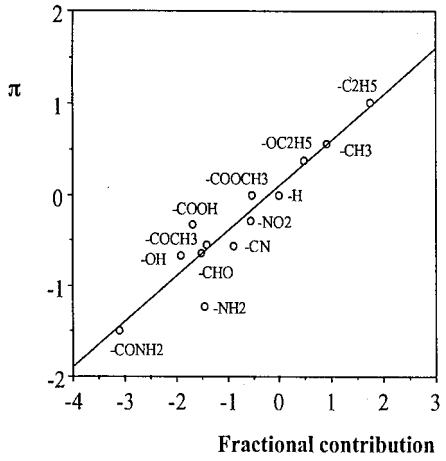

Figure 10. Relationship between fractional chloroform/water partition coefficients (relative to the partition coefficient of benzene) determined at the QM HF/6-31G(d) level and empirical octanol/water π values for selected substituents. The regression equation is $y = 0.50 \times + 0.09$ ($r^2 = 0.88$).

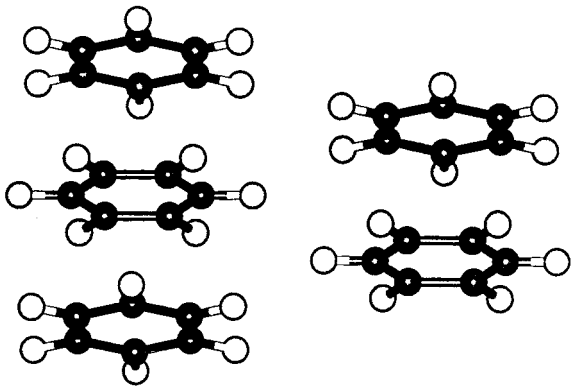

Figure 11. Structures of the benzene dimer and trimer used in this study (see text).

energy of solvation of the isolated molecule. Within the framework of empirical fractional models, the contribution of benzene to solvation would be a priori the same for the isolated molecule or for every benzene molecule in the stacked complexes. Theoretical calculations, however, show that every benzene in a dimer contributes to solvation less than the isolated molecule, as a consequence of the decrease in the solvent accessible surface upon dimerization. This effect is even more evident for the central molecule in the trimer, since its contribution is nearly one third of the solvation free energy determined for the isolated monomer in chloroform and is even positive in water.

Table 4. Fractional free energies of solvation (kcal/mol) in water and chloroform determined at the AM1 level for the monomer, dimer and trimer (stacked complexes) of benzene

Solvent	System	ΔG_{sol} (total)	ΔG_{sol} (monomer)
Water	monomer	−0.90	−0.90
	dimer	−1.20	−0.60
	trimer	−1.38	−0.87[a], 0.36[b]
Chloroform	monomer	−5.82	−5.82
	dimer	−8.78	−4.39
	trimer	−11.16	−4.65[a], −1.86[b]

[a]Values for the terminal benzene monomers in the trimer.
[b]Values for the central benzene in the trimer (Figure 11).

Conclusions

The method presented here allows the rigorous partition of free energies of solvation into surface elements. These surface contributions can then be added to determine atom or group fractional contributions to the total free energy of solvation. Combination of fractional contributions to solvation in different solvents allows us to determine the fractional contributions to the transfer free energy. This allows for 3-D representations of the hydrophobic/hydrophilic characteristics of molecules. In addition, the method allows for prediction of the effect that a chemical modification would have on the hydrophobicity/hydrophilicity of a different region of the molecule.

The method is rigorous only at the QM ab initio level, but can also provide reasonable values at the semiempirical or even *quasi-classical* levels. It can then be used to study the hydrophilic/hydrophobic characteristics of medium and large molecules. This feature, as well as the ability of the method to represent 3-D solvation properties of molecules, suggest that the partitioning scheme presented here migth be valuable in molecular modeling studies.

Acknowledgements

We thank Prof. J. Tomasi for a copy of his MST routines, which were modified by us to perform these calculations. We also thank Profs. J. Tomasi and C. J. Cramer for providing several references prior to their publication, and Prof. F. Gago for valuable suggestions. This work has been supported by the Centre de Supercomputació de Catalunya (CESCA; Mol. Recog. Project), and by the Spanish DGICYT: PB96-1005

and PB97-0908. X.B. acknowledges the Ministerio de Educación y Cultura for a FPI-fellowship.

References

1. Hansch, C., Maloney, P.P., Fujita, T. and Mui, R., Nature, 194 (1963) 178.
2. Hansch, C., Acc. Chem. Res., 2 (1969) 232.
3. Leo, A., Hansch, C. and Elkins, D., Chem Rev., 71 (1971) 525.
4. Martin, Y.C., Quantitative Drug Design. A Critical Introduction, Marcel Dekker, New York, NY, 1978.
5. Hansch, C. and Leo, A., Exploring QSAR: Fundaments and Applications in Chemistry and Biology, ACS, Washington, DC, 1995.
6. Hansch, C. and Fujita, T., J. Am. Chem. Soc., 86 (1964) 1616.
7. Eisenberg, D. and McLachlan, A.D., Nature, 319 (1986) 199.
8. Audry, E., Dubost, J.P., Colleter, J.C. and Dallet, P., Eur. J. Med. Chem.-Chim. Ther., 21 (1986) 71.
9. Fauchère, J.L., Quarendon, P. and Kaetterer, L., J. Mol. Graphics, 6 (1988) 202.
10. Furet, P., Sele, A. and Cohen, N.C., J. Mol. Graphics, 6 (1988) 182.
11. Hansch, C. and Leo, A., Substituent Constants for Correlation Analysis in Chemistry and Biology, John Wiley and Sons, New York, NY, 1979.
12. Nys, G.G. and Rekker, R.F., Chim. Ther., 8 (1973) 521.
13. Rekker, R.F., The Hydrophobic Fragmental Constant. Elsevier, Amsterdam, 1977.
14. Suzuki, Y. and Kudo, Y., J. Comput.-Aided Mol. Design, 4 (1990) 155.
15. Bodor, N., Gabany, Z. and Wong, C.K., J. Am. Chem. Soc., 111 (1989) 3783.
16. Ghose, A.K. and Crippen, G.M., J. Comput. Chem., 7 (1986) 565.
17. Viswanadhan, V.N., Ghose, A.K., Revenkar, G.R. and Robins, R., J. Chem. Inf. Comput. Sci., 29 (1989) 163.
18. Klopman, G. and Wang, S., J. Comput. Chem., 12 (1991) 1025.
19. Meylan, W.M. and Howard, P.H., J. Pharm. Sci., 84 (1995) 83.
20. Mannhold, R. and Dross, K., Quant. Struct.-Act. Relat., 15 (1996) 403, and references therein.
21. Wang, R., Fu, Y. and Lai, L., J. Chem. Inf. Comput. Sci., 37 (1997) 615.
22. Gombar, V. and Enslein, K., J. Chem. Inf. Comput. Sci., 36 (1996) 1127, and references therein.
23. Bask, S.C., Gute, B.D. and Grunwald, G.D., J. Chem. Inf. Comput. Sci., 36 (1996) 1054.
24. van de Waterbeemd, H. and Mannhold, R., Quant. Struct.-Act. Relat., 15 (1996) 410, and references therein.
25. Convard, T., Dubost, J.P., Le Solleu, H. and Kummer, E., Quant. Struct.-Act. Relat., 13 (1994) 34.
26. Haeberlein, M. and Brinck, T., J. Chem. Soc., Perkin Trans. 2, (1997) 289.
27. Bodor, N. and Buchwald, P., J. Phys. Chem. B., 101 (1997) 3404.
28. Du, Q. and Arteca, G.A., J. Comput.-Aided Mol. Design, 10 (1996) 13.
29. Lien, E.J., Gao, H., Wang, F. and Shinouda, H.G., Quant. Struct.-Act. Relat., 12 (1993) 158.
30. Orozco, M., Alhambra, C., Barril, X., López, J.M., Busquets, M.A. and Luque, F.J., J. Mol. Model., 2 (1996) 1.
31. Jorgensen, W.L., In Van Gunsteren, W.F. and Weiner, P.K. (Eds.) Computer Simulation of Biomolecular Systems. Theoretical and Experimental Applications, ESCOM, Leiden, 1989, pp. 60–72.
32. Rivail, J.L. and Rinaldi, D., In Leszcynski, J. (Ed.) Computational Chemistry, Review of Current Trends, World Scientific Publishing, Singapore, 1996, pp. 139–169.
33. Tomasi, J. and Persico, M., Chem. Rev., 94 (1994) 2027.
34. Cramer, C.J. and Truhlar, D.G., In Tapia, O. and Bertraán, J. (Eds.) Solvent Effects and Chemical Reactivity, Kluwer Academic Publishers, Dordrecht, 1996, pp. 1–80.
35. Barone, V., Cossi, M. and Tomasi, J., J. Comput. Chem., 19 (1998) 404.
36. Sitkoff, D., Sharp, K.A. and Honig, B., J. Phys. Chem., 98 (1994) 1978.
37. Still, W.C., Tempczyk, A., Hawley, R.C. and Hendrickson, T., J. Am. Chem. Soc., 112 (1990) 6127.
38. Luty, B.A., Wasserman, Z.R., Stouten, P.F.W., Hodge, C.N., Zacharias, M. and McCammon, J.A., J. Comput. Chem., 16 (1995) 454.
39. DELPHI computer program, Biosym Technologies, San Diego, CA, 1992.
40. Giesen, D.J., Gu, M.Z., Cramer, C.J. and Truhlar, D.G., J. Org. Chem., 61 (1996) 8720.
41. Giesen, D.J., Hawkins, G.D., Liotard, D.A., Cramer, C.J. and Truhlar, D.G., Theor. Chem. Acc., 98 (1997) 85.
42. Luque, F.J., Bachs, M., Alemán, C. and Orozco, M., J. Comput. Chem., 17 (1996) 806.
43. Luque, F.J., Zhang, Y., Alemán, C., Bachs, M., Gao, J. and Orozco, M., J. Phys. Chem., 100 (1996) 4269.
44. Miertus, S., Scrocco, E. and Tomasi, J., Chem. Phys., 55 (1981) 117.
45. Miertus, S. and Tomasi, J., Chem. Phys., 65 (1982) 239.
46. Pierotti, R.A., Chem. Rev., 76 (1976) 717.
47. Claverie, P., In Pullman, B. (Ed.) Intermolecular Interactions: from Diatomics to Biomolecules, Wiley, Chichester, 1978, p. 71.
48. Bachs, M., Luque, F.J. and Orozco, M., J. Comput. Chem., 15 (1994) 446.
49. Hoshi, H., Sakurai, M., Inoue, Y. and Chûjô, R., J. Mol. Struct. (Theochem), 180 (1988) 267.
50. Coitiño, E.L., Tomasi, J. and Cammi, R., J. Comput. Chem., 16 (1995) 20.
51. Cammi, R. and Tomasi, J., J. Comput. Chem., 16 (1995) 1449.
52. Cammi, R. and Tomasi, J., J. Chem. Phys., 101 (1994) 3888.
53. Cammi, R. and Tomasi, J., J. Chem. Phys., 101 (1994) 7495.
54. Luque, F.J., Bofill, J.M. and Orozco, M., J. Chem. Phys., 103 (1995) 10183.
55. Ángyán, J.G., J. Chem. Phys., 107 (1997) 1291.
56. Luque, F.J., Bofill, J.M. and Orozco, M., J. Chem. Phys., 107 (1997) 1293.
57. Luque, F.J. and Orozco, M., J. Phys. Chem., 101 (1997) 5573.
58. Orozco, M., Roca, R., Alemán, C., Busquets, M.A., López, J.M. and Luque, F.J., J. Mol. Struct. (Theochem), 371 (1996) 269.
59. Colominas, C., Orozco, M., Luque, F.J., Borrell, J.I. and Teixidó, J., J. Org. Chem., 63 (1998) 4947.
60. Tomasi, J., Bonaccorsi, R., Cammi, R. and Olivares del Valle, F.J., J. Mol. Struct. (Theochem), 234 (1991) 401.
61. Olivares del Valle, F.J. and Aguilar, M.A., J. Comput. Chem., 13 (1992) 115.
62. Luque, F.J., Negre, M.J. and Orozco, M., J. Phys. Chem., 97 (1993) 4386.
63. Orozco, M. and Luque, F.J., Chem.Phys., 182 (1994) 237.

64. Luque, F.J., Bachs, M. and Orozco, M., J. Comput. Chem., 15 (1994) 847.
65. Orozco, M., Bachs, M. and Luque, F.J., J. Comput. Chem., 16 (1995) 563.
66. Giesen, D.J., Chambers, C.C., Cramer, C.J. and Truhlar, D.G., J. Phys. Chem. B., 101 (1997) 5084.
67. Giesen, D.J., Chambers, C.C., Hawkins, G.D., Cramer, C.J. and Truhlar, D.G., In Irikura, K. and Frurip, D.J. (Eds.), Computational Thermochemistry: Prediction and Estimation of Molecular Thermodynamics, ACS Symposium Series, American Chemical Society, Washington, DC, 1998, p. 285.
68. Hawkins, G.D., Liotard, D.A., Cramer, C.J. and Truhlar, D.G., J. Org. Chem., 63 (1998) 4305.
69. Chambers, C.C., Giesen, D.J., Hawkins, G.D., Vaes, W.H., Cramer, C.J. and Truhlar, D.G., In Truhlar, D.G., Howe, W.J., Blaney, J.M., Hopfinger, A.J. and Dammkoehler, R.A (Eds.) Computer-Assisted Drug Design, Springer, New York, NY, 1998.
70. Peterson, M. and Poirier, R., MONSTERGAUSS; Dept. of Chemistry, Univ. of Toronto, Canada; version modified by Cammi, R., Bonaccorsi, R. and Tomasi, J., University of Pisa, Pisa 1987. Modified by Luque, F.J. and Orozco, M., University of Barcelona, Barcelona 1997.
71. Stewart, J.J.P., MOPAC 93 Rev 2. Fujitsu Limited, 1993. Modified by Luque, F.J. and Orozco, M., University of Barcelona, Barcelona 1997.
72. Luque, F.J. and Orozco, M., MOPETE/MOPFIT, University of Barcelona, Barcelona 1998.
73. INSIGHT-II computer program, Biosym Technologies, San Diego, CA, 1994.
74. Alhambra, C., Luque, F.J. and Orozco, M., J. Comput. Chem., 15 (1994) 12.
75. Dewar, M.J.S., Zoebisch, E.G., Horsley, E.F. and Stewart, J.J.P., J. Am. Chem. Soc., 107 (1985) 3902.
76. Stewart, J.J.P., J. Comput. Chem., 10 (1989) 209.
77. Backbro, K., Lowgren, S., Osterlund, K., Atepo, J., Unge, T., Hulten, J., Bonham, N.M., Schaal, W., Karlen, A. and Hallberg, A., J. Med. Chem., 40 (1997) 898.
78. Lide, D.R. (Ed.) Handbook of Organic Solvents, CRC Press, Boca Raton, FL, 1995.